Increased sympathetic outflow in juvenile rats submitted to chronic intermittent hypoxia correlates with enhanced expiratory activity

Daniel B. Zoccal[1], Annabel E. Simms[2], Leni G. H. Bonagamba[1], Valdir A. Braga[1], Anthony E. Pickering[2], Julian F. R. Paton[2] and Benedito H. Machado[1]

[1]*Department of Physiology, School of Medicine of Ribeirão Preto, University of São Paulo, Ribeirão Preto, SP, Brazil*
[2]*Department of Physiology and Pharmacology, Bristol Heart Institute, School of Medical Sciences, University of Bristol, Bristol BS8 1TD, UK*

Chronic intermittent hypoxia (CIH) in rats produces changes in the central regulation of cardiovascular and respiratory systems by unknown mechanisms. We hypothesized that CIH (6% O_2 for 40 s, every 9 min, 8 h day^{-1}) for 10 days alters the central respiratory modulation of sympathetic activity. After CIH, awake rats ($n = 14$) exhibited higher levels of mean arterial pressure than controls (101 ± 3 *versus* 89 ± 3 mmHg, $n = 15$, $P < 0.01$). Recordings of phrenic, thoracic sympathetic, cervical vagus and abdominal nerves were performed in the *in situ* working heart–brainstem preparations of control and CIH juvenile rats. The data obtained in CIH rats revealed that: (i) abdominal (Abd) nerves exhibited an additional burst discharge in late expiration; (ii) thoracic sympathetic nerve activity (tSNA) was greater during late expiration than in controls (52 ± 5 *versus* 40 ± 3%; $n = 11$, $P < 0.05$; values expressed according to the maximal activity observed during inspiration and the noise level recorded at the end of each experiment), which was not dependent on peripheral chemoreceptors; (iii) the additional late expiratory activity in the Abd nerve correlated with the increased tSNA; (iv) the enhanced late expiratory activity in the Abd nerve unique to CIH rats was accompanied by reduced post-inspiratory activity in cervical vagus nerve compared to controls. The data indicate that CIH rats present an altered pattern of central sympathetic–respiratory coupling, with increased tSNA that correlates with enhanced late expiratory discharge in the Abd nerve. Thus, CIH alters the coupling between the central respiratory generator and sympathetic networks that may contribute to the induced hypertension in this experimental model.

(Received 17 March 2008; accepted after revision 30 April 2008; first published online 1 May 2008)
Corresponding author B. H. Machado: Department of Physiology, School of Medicine of Ribeirão Preto, University of São Paulo, 14049-900, Ribeirão Preto, SP, Brazil. Email: bhmachad@fmrp.usp.br

Chronic intermittent hypoxia (CIH) is observed in the pathophysiological state of obstructive sleep apnoea (OSA). As a consequence of the long-term exposure to intermittent hypoxia, OSA patients are at increased risk of substantial dysfunctions in the cardiovascular system including the development of sustained hypertension (Hoffman *et al.* 2004; Caples *et al.* 2005). Clinical (Narkiewicz & Somers, 1997; Leuenberger *et al.* 2005) and experimental (Zoccal *et al.* 2007*b*) evidence indicates increased sympathetic outflow as the main cause for the sustained hypertension after CIH. However, the relationship between CIH and the mechanisms underpinning excessive sympathetic activity are not understood completely. Studies from our laboratory documented that juvenile rats submitted to CIH exhibited a greater sympathoexcitatory response to peripheral chemoreceptor activation (Braga *et al.* 2006), suggesting that the central processing of the sympathoexcitatory component of the chemoreflex is enhanced. This possibility is supported by studies in CIH rats showing important functional changes in pontine–medullary areas involved in the generation and respiratory modulation of sympathetic nerve activity (Greenberg *et al.* 1999; Reeves *et al.* 2003, 2006). In addition to changes in the sympathetic nervous system, considerable alterations are also observed in the respiratory system of rats submitted to CIH, such as enhanced long-term facilitation of respiratory motor activity (McGuire *et al.* 2003) and an augmented ventilatory response to hypoxia (Ling *et al.* 2001; Braga

J. F. R. Paton and B. H. Machado are joint last authors.

 DOI: 10.1113/jphysiol.2008.154187

et al. 2006) suggesting that CIH changes brainstem respiratory network function in rats (Reeves *et al.* 2006; Kline *et al.* 2007).

It is well known that cardiovascular sympathetic activity is markedly modulated by central respiratory activity (Adrian *et al.* 1932; Zhou & Gilbey, 1992; Pilowsky, 1995; Malpas, 1998). The pattern of coupling between respiratory and sympathetic activities varies according to the species (Häbler *et al.* 1994), the nerve recorded (Jänig & Häbler, 2003) and the state of the preparation (Gilbey *et al.* 1986; Dick *et al.* 2004), but the predominant patterns include a peak of sympathetic nerve discharge coincident with either inspiration or immediately after inspiration in the post-inspiratory/early expiratory period (Malpas, 1998). There is evidence that part of the respiratory modulation of sympathetic activity is a consequence of afferent feedback from pulmonary stretch receptors (Anrep *et al.* 1936; Boczek-Funcke *et al.* 1992). However, several studies have documented that the influence of respiratory rhythm on sympathetic activity persists after vagotomy indicating a central coupling between respiratory and presympathetic neurons located in the brainstem (Barman & Gebber, 1980; Haselton & Guyenet, 1989; Häbler *et al.* 1996; Zhong *et al.* 1997). Therefore, considering the evidence that CIH affects brainstem control of both the respiratory and sympathetic nervous systems, we tested the hypothesis that CIH changes the temporal profile of coupling between centrally generated respiratory activities and sympathetic activities in juvenile rats. To test this, we used an *in situ* and artificially perfused working heart–brainstem preparation of juvenile rats (Pickering & Paton, 2006; Simms *et al.* 2007) since it generates robust sympathetic activity, which is respiratory modulated, and is free from the depressant effects of anaesthesia.

Methods

Animals

Juvenile male Wistar rats (19–21 days) were divided into two experimental groups: rats exposed to chronic intermittent hypoxia (CIH, $n = 40$) and rats maintained under normoxic conditions (control, $n = 41$). These rats were obtained from the Animal Care of the University of São Paulo at Ribeirão Preto, Brazil. All experimental approaches were approved by the Ethical Committee on Animal Experimentation of the School of Medicine of Ribeirão Preto, University of São Paulo (protocol 019/2006).

Chronic intermittent hypoxia

Both CIH and control rats were housed in collective cages and maintained inside Plexiglas chambers (volume, 210 l) equipped with gas injectors as well as sensors of O_2, CO_2, humidity and temperature. The CIH group was exposed to a protocol of 5 min of normoxia (fraction of inspired O_2, F_{IO_2}, of 20.8%) followed by 4 min of pure N_2 injection to reduce the F_{IO_2} from 20.8 to 6%, remaining at this level for 40 s. After this hypoxic period, pure O_2 was injected into the chamber to return the F_{IO_2} back to 20.8%. This 9 min cycle was repeated 8 h a day (from 9.30 am to 5.30 pm) for 10 days. During the remaining 16 h, the animals were maintained at a F_{IO_2} of 20.8%. The injections of N_2 and O_2 (White Martins, Sertãozinho, Brazil) into the chamber were regulated by a solenoid valve system whose opening–closing control was operated by a computerized system (Oxycycler, Biospherix, USA). In an identical chamber in the same room, the control group of rats was exposed to a F_{IO_2} of 20.8% 24 h a day for 10 days. The control rats were also exposed to a similar valve noise due to the frequent injection of O_2 to maintain the F_{IO_2} at 20.8%. In both CIH and control chambers, the gas injections were performed at the upper level of the chamber in order to avoid direct jets of gas impacting on the animals, which could cause stress.

Mean arterial pressure and heart rate measurements

At the end of the experimental protocol some of the CIH ($n = 14$) and control rats ($n = 15$) were anaesthetized with tribromoethanol (250 mg kg^{-1}, I.P.; Aldrich, Milwaukee, WI, USA) and a catheter was inserted into the abdominal aorta through the femoral artery (PE-10 connected to PE-50 tubing, Clay Adams, Parsippany, NJ, USA) for arterial pressure measurement. The catheter was tunnelled subcutaneously and exteriorized through the back of the neck. Twenty-four hours later, when the rats were completely recovered from the surgery and adapted to the environment of the recording room, the arterial catheter was connected to a pressure transducer (MLT0380, ADInstruments, NSW, Australia), and in turn, to an amplifier (Bridge Amp, ML221, ADInstruments, NSW, Australia). The pulsatile arterial pressure signals were acquired by a data acquisition system (PowerLab 4/25, ML845, ADInstruments) and recorded on the hard drive of a computer using appropriate software (Chart Pro, ADInstruments). The values of diastolic, mean and systolic arterial pressure and heart rate were then determined from the signals of pulsatile arterial pressure. The cardiovascular parameters were recorded in conscious freely moving rats under normoxic conditions for 45–60 min and the data obtained during the last 30 min were considered for analysis.

Working heart–brainstem preparation (WHBP)

CIH ($n = 26$) and control rats ($n = 26$) were deeply anaesthetized with halothane (AstraZeneca do Brasil Ltda.,

Cotia, SP, Brazil) such that the withdrawal responses to noxious pinching of the tail and paw were absent. The animals were then transected caudal to the diaphragm, exsanguinated and submerged in a cooled Ringer solution. They were decerebrated at the precollicular level to make insentient, and skinned. The descending aorta was isolated and the lungs removed. In some CIH ($n = 5$) and control preparations ($n = 3$) all the afferents arising from carotid bifurcations were mechanically removed in order to disrupt the carotid chemoreceptor afferents. The efficacy of peripheral chemoreceptor denervation was confirmed by the absence of autonomic and respiratory responses to peripheral chemoreceptor activation with potassium cyanide (data not shown). This procedure also removed the afferents from carotid baroreceptors. Preparations were then transferred to a recording chamber, the descending aorta was cannulated and perfused retrogradely with Ringer solution (in mM: NaCl, 125; $NaHCO_3$, 24; KCl, 5; $CaCl_2$, 2.5; $MgSO_4$, 1.25; KH_2PO_4, 1.25; dextrose, 10) containing 1.25% Ficoll (an oncotic agent; Sigma, St Louis, MO, USA) and a neuromuscular blocker (vecuronium bromide, 3–4 μg ml^{-1}, Cristália Produtos Qu'micos Farmacêuticos Ltda, São Paulo, Brazil), using a roller pump (Watson-Marlow 502s, Falmouth, Cornwall, UK) via a double-lumen cannula. The perfusion pressure was maintained in the range 50–70 mmHg by adjusting the flow between 21 and 25 ml min^{-1} and by adding vasopressin (600–1200 pM, Sigma) to the perfusate, as previously described (Pickering & Paton, 2006). The perfusate was continuously gassed with 5% CO_2 and 95% O_2 (White Martins, Sertãozinho, Brazil), warmed to 31–32°C (temperature measured at the point of entry into the aorta) and filtered using a nylon mesh (pore size: 25 μm, Millipore, Billirica, MA, USA).

Data recordings and analyses

Numerous combinations of cardiorespiratory motor nerves were isolated and recorded with up to three being recorded simultaneously. All nerve recordings were obtained using glass suction electrodes held in a micromanipulator (Narishige, Tokyo, Japan). Phrenic nerve (left) discharge was recorded from its central end using a unipolar electrode and its rhythmic ramping activity gave a continuous physiological index of preparation viability. The electrocardiogram was visible on the phrenic recording and using a window discriminator the R-wave was captured and the inter-R wave interval displayed as heart rate (HR). The cervical vagus nerve (left) was cut distally and its central activity recorded. The efferent activity of the left thoracic sympathetic nerve (tSNA) was recorded from the sympathetic chain at the level of T8–T12. An abdominal nerve was isolated from the abdominal muscles on the right at thoracic–lumbar level, cut distally and its activity recorded. The activities of cervical vagus, thoracic sympathetic and abdominal nerves were recorded using bipolar glass suction electrodes. All the signals were amplified, band-pass filtered (0.5–5 kHz) and acquired in an A/D converter (CED 1401, Cambridge Electronic Design, CED, Cambridge, UK) to a computer using Spike 2 software (CED). The frequency of phrenic discharge was determined by the time interval between consecutive phrenic bursts and the analyses of the activities of cervical vagus, thoracic sympathetic and abdominal nerves were carried out on the rectified and integrated signals (time constant of 100 ms). All the analyses were performed off-line using Spike 2 software with custom-written scripts.

Analysis of respiratory–sympathetic activity coupling

Phrenic-triggered averaging of integrated tSNA was carried out using the same amplification and band-pass filter parameters. These averages were taken from 10 integrated phrenic cycles (time constant of 100 ms). The averaged tSNA was divided into four parts: late expiration, inspiration (I), post-inspiration (PI) and mid-expiration. The time duration of late expiration, I, PI and mid-expiration was based on the duration of the inspiratory phrenic burst (i.e. time to the peak of the ramp). To analyse the pattern of tSNA during the respiratory cycle, the peak activity observed during I was considered to be 100% and the activities observed during I, PI, mid- and late-expiration periods were the average values obtained, normalized by the peak of activity observed during I. The noise level, which was considered as 0%, was determined 10–20 min after ceasing arterial perfusion at the end of each experiment and subtracted from tSNA. This analysis was applied for each preparation and the data obtained were pooled across preparations, i.e. CIH ($n = 9$) and control rats ($n = 11$) with intact peripheral chemoreceptors, and CIH ($n = 5$) and control rats ($n = 3$) with denervated peripheral chemoreceptors.

Analysis of vagus nerve activity

Phrenic-triggered averaging of integrated cervical vagus nerve activity over 10 respiratory cycles was subsequently divided into three parts: inspiratory (coincident with inspiratory phrenic discharge), early post-inspiratory (early PI, duration of which was defined by the duration of the preceding phrenic burst as described above) and late-PI (i.e. all remaining PI activity). To assess the activity in the inspiratory and post-inspiratory phases of vagus activity, areas under the curve were quantified in each part and normalized by the total area, i.e. sum of areas obtained in inspiratory, early PI and late-PI. This analysis was applied for each preparation and the data obtained were pooled

together and compared between CIH ($n = 10$) and control groups ($n = 10$).

Analysis of cross-correlation

Cross-correlation analyses were performed between phrenic *versus* abdominal activities and between tSNA *versus* abdominal activities in control ($n = 5$) and CIH ($n = 5$) groups over 10 phrenic cycles. The peak activity of the abdominal nerve was used as a trigger (time 0) for all correlograms. The results are expressed as the correlation coefficient (r), in accordance with Cohen (1988), ranging from 1 (correlated waves) through 0 (uncorrelated) to –1 (correlated but inverted waves). In all cases, neural signals were smoothed using a time constant of 100 ms. This analysis was performed offline using Spike 2 software.

Statistical analyses

The results were expressed as mean ± standard error of the mean and compared using Student's unpaired t test. The comparisons were carried out on GraphPad Prism software (GraphPad Software, version 4) and differences were considered significant at $P < 0.05$.

Results

Body weight after CIH exposure

Both juvenile CIH ($n = 40$) and control rats ($n = 41$) entered the hypoxic and control chambers with similar body weight (46 ± 2 *versus* 44 ± 2 g). At the end of the experimental protocol, the rats submitted to CIH for 10 days exhibited a lower body weight compared to control rats (79 ± 3 *versus* 98 ± 4 g, $P < 0.0001$).

Cardiovascular parameters after CIH exposure measured in conscious rats *in vivo*

Conscious CIH rats ($n = 14$) exhibited significantly higher diastolic (80 ± 2 *versus* 72 ± 2 mmHg, $P < 0.05$, Fig. 1*A*), systolic (129 ± 3 *versus* 120 ± 3 mmHg, $P < 0.05$, Fig. 1*B*) and mean arterial pressure (101 ± 3 *versus* 89 ± 3 mmHg, $P < 0.01$, Fig. 1*C*), with no changes in the differential pulse pressure (49 ± 2 *versus* 48 ± 2 mmHg, Fig. 1*D*) relative to controls ($n = 15$). There was no difference in baseline heart rate between CIH and control rats (511 ± 15 *versus* 495 ± 11 beats min^{-1}).

Cardiovascular parameters after CIH exposure measured in the WHBP

The perfusion pressure of WHBP of CIH ($n = 26$) and control rats ($n = 26$) was set to similar levels (66 ± 2 *versus* 67 ± 2 mmHg) by adjusting the perfusate flow rate between 21 and 25 ml min^{-1} and by adding vasopressin (AVP) to the perfusate (see Methods). In this regard, we observed that WHBP of CIH rats required a higher concentration of AVP (1000–1200 pM) than controls (600–800 pM) to match perfusion pressure at a given perfusion rate. In addition, when the same dose of AVP was added to the perfusate (600 pM), the perfusion pressure increased less in CIH than control WHBP (4 ± 1 *versus* 14 ± 2 mmHg, $P < 0.01$). To exclude the possibility

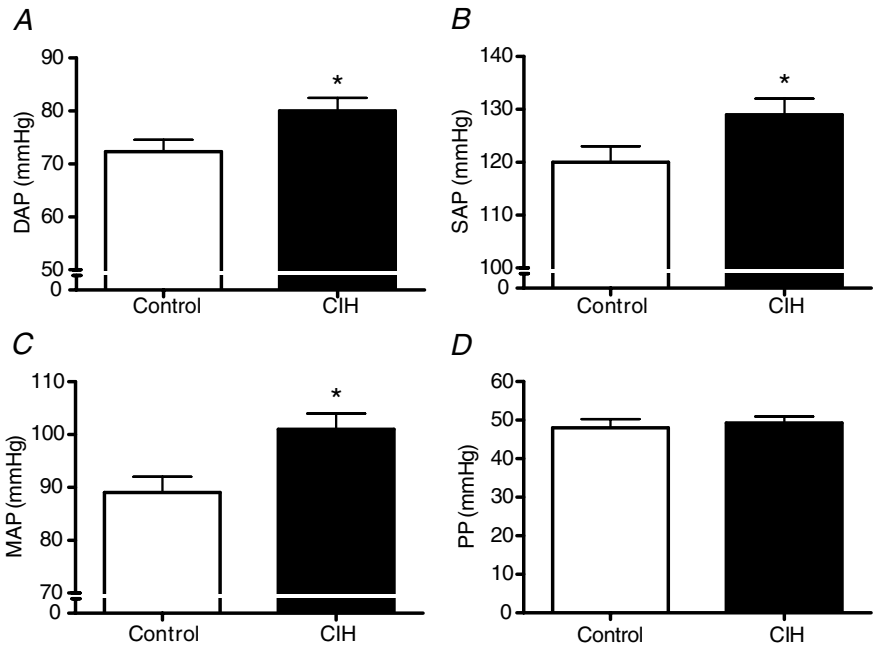

Figure 1. Cardiovascular parameters measured in awake juvenile control and chronic intermittent hypoxia-treated (CIH) rats
Diastolic (DAP, *A*), systolic (SAP, *B*) and mean arterial pressure (MAP, *C*), and pulse pressure (PP, *D*) of control ($n = 15$) and CIH-treated rats ($n = 14$). * Different from control group, $P < 0.05$.

that the higher concentration of AVP required by WHBPs of CIH rats might contribute to the respiratory and sympathetic alterations observed in this experimental group, WHBPs of naive rats ($n = 4$) received the same concentration of AVP used in CIH rats and the records showed no changes in the basal pattern of sympathetic and respiratory activities and their coupling (data not shown). In relation to baseline heart rate, no differences were observed between CIH ($n = 21$) and control rats ($n = 24$) with intact peripheral chemoreceptors (422 ± 19 *versus* 425 ± 11 beats min^{-1}). Similarly, CIH ($n = 5$) and control rats ($n = 3$) with denervated peripheral chemoreceptors exhibited similar baseline perfusion pressures (at comparable flow rates and vasopressin administration) and heart rate (404 ± 9 *versus* 406 ± 31 beats min^{-1}).

Respiratory pattern after CIH exposure measured in the WHBP

Both CIH ($n = 21$) and control WHBPs ($n = 24$) with intact peripheral chemoreceptors showed similar phrenic discharge duration (511 ± 26 *versus* 541 ± 25 ms) and frequency (0.32 ± 0.03 *versus* 0.34 ± 0.02 Hz). Likewise, CIH ($n = 5$) and control rats ($n = 3$) with denervated peripheral chemoreceptors showed no statistical difference in phrenic discharge duration (1370 ± 209 *versus* 745 ± 82 ms) and frequency (0.21 ± 0.01 *versus* 0.22 ± 0.06 Hz). In comparison with control and CIH groups with intact peripheral chemoreceptors, both control and CIH-denervated groups showed longer phrenic duration (CIH: 1370 ± 209 *versus* 511 ± 26 ms; control: 745 ± 82 *versus* 541 ± 25 ms; $P < 0.05$), with no statistical difference in relation to phrenic frequency.

In relation to the expiratory activity, analyses were performed between abdominal and cervical vagus basal nerve recordings of control and CIH rats. In all preparations of control rats ($n = 7$), the abdominal activity showed a relatively small post-inspiratory-related discharge, followed by irregular low amplitude activity during the remaining expiratory phase and an inhibition coincident with the phrenic discharge (Figs 2 and 5). In addition, the vagus activity in controls ($n = 10$) exhibited inspiratory (coincident with phrenic discharge) and post-inspiratory activities followed by quiescence prior to the next phrenic burst (Fig. 3). In the CIH group ($n = 8$), the expiratory activity pattern of the abdominal nerve was markedly different relative to controls. In 7 out of 8 preparations, the abdominal nerve exhibited a novel burst that occurred during late expiration; the small peak of activity in post-inspiration remained as did the inhibition during inspiration (Figs 2 and 5). This indicated that in CIH rats, but not controls, there was evidence for enhanced/forced expiratory activity. Besides, early PI activity, but not late-PI activity recorded from the cervical vagus was also reduced in CIH ($n = 10$) when compared to controls ($n = 10$; Fig. 3).

Respiratory–sympathetic coupling after CIH exposure in the WHBP

In both CIH and control rats, tSNA showed clear respiratory modulation with peak activity coincident with the end of inspiratory phrenic discharge and start of expiration (Fig. 4, upper panels). During the PI period, tSNA declined reaching its lowest level during mid-expiration in both animal groups (Fig. 4, upper panels). In contrast to control rats, CIH animals ($n = 9$) exhibited a higher level of tSNA during late expiration (52 ± 5 *versus* $40 \pm 3\%$, $P < 0.05$) – a time when late expiratory activity was expressed in the abdominal nerve of these animals. However, no significant difference in tSNA was observed during I (79 ± 3 *versus* $71 \pm 3\%$),

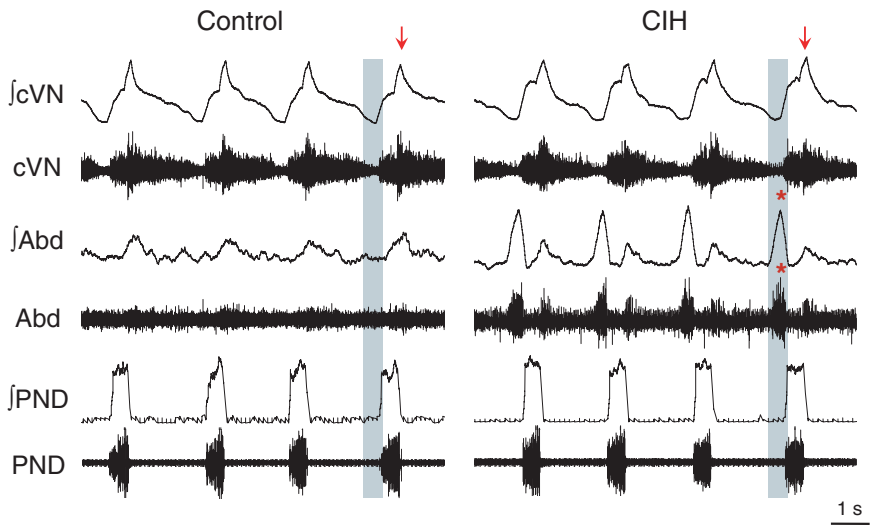

Figure 2. Raw and integrated (∫) activities of motor nerves recorded simultaneously from cervical vagus (cVN), abdominal (Abd) and phrenic nerve (PND) from one representative working heart–brainstem preparation (WHBP) in the control and CIH groups
The shaded grey area in the recordings indicates the late expiratory phase of the respiratory cycle and the arrows in the cVN indicate the beginning of post-inspiratory activity. Note the emergence of late-expiratory bursts in the Abd of the CIH rat (*).

PI (35 ± 4 *versus* $35 \pm 4\%$) and mid-expiration (42 ± 5 *versus* $38 \pm 3\%$) in comparison to control rats ($n = 11$; middle panels of Fig. 4). Control rats with denervated peripheral chemoreceptors ($n = 3$) exhibited a similar pattern of respiratory modulation of tSNA to control rats with intact peripheral chemoreceptors. Similarly, CIH rats with denervated peripheral chemoreceptors ($n = 5$) again presented a higher tSNA during late expiration (58 ± 3 *versus* $44 \pm 1\%$, $P < 0.05$) but similar activity during the other respiratory periods when compared to CIH rats with intact peripheral chemoreceptors (I: 80 ± 2 *versus* $77 \pm 2\%$; PI: 38 ± 7 *versus* $27 \pm 6\%$; mid-expiration: 49 ± 6 *versus* $34 \pm 6\%$, lower panel of Fig. 4). Thus, the central respiratory coupling of tSNA and the enhancement seen during the late expiratory period observed in CIH rats were both independent of peripheral chemoreceptor input. In addition, the simultaneous recordings of tSNA and abdominal nerve showed that the increased late-expiratory sympathetic activity of CIH rats is associated with enhanced/forced expiratory activity, as shown in Fig. 5.

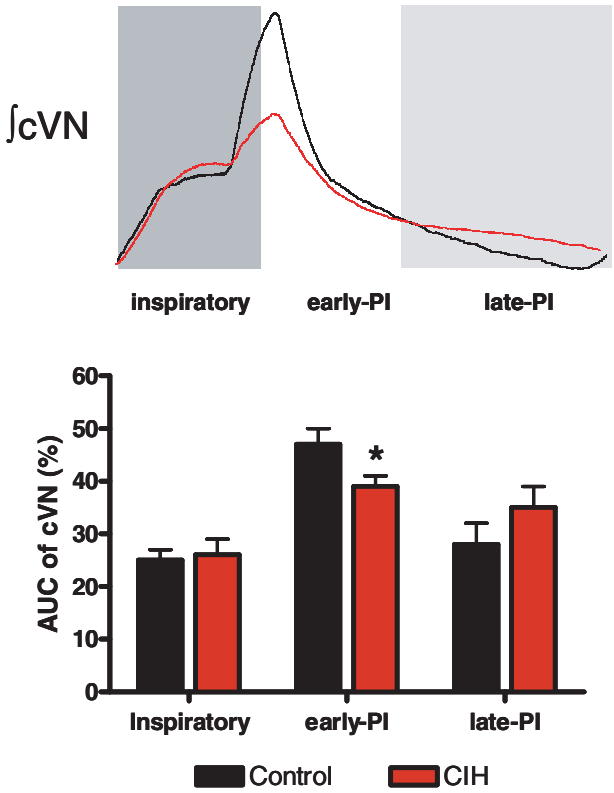

Figure 3. Analysis of cervical vagus nerve activity (cVN) in control and CIH-treated rats
Upper panel: phrenic-triggered average of integrated cervical vagus nerve ($\int$cVN), obtained from 10 phrenic cycles in one representative WHBP of control and CIH groups. The early post-inspiratory activity (early PI) of cVN observed in CIH rats was reduced in relation to controls, but there was no change in late-PI and inspiratory activities. Lower panel: mean values of the area under the curve (AUC) of the different components of cVN in control ($n = 10$) and CIH groups ($n = 10$). The values were normalized by the total cVN area (equivalent to the sum of the areas of the three cVN components). * Different from control group, $P < 0.05$.

Cross-correlation between abdominal outflow and sympathetic activity

Representative correlograms from one control (left) and one CIH (right) WHBP are shown in Fig. 6. In this figure, tSNA (upper panels) and phrenic nerve activity (middle panels) are triggered from the peak of abdominal nerve activity (lower panels). In this control group simultaneous recording of abdominal and tSNA were performed in five WHBPs. The maximal peak of abdominal activity (at time 0) correlated with post-inspiration (i.e. immediately after phrenic discharge) whereas tSNA occurred during the latter stages of the phrenic burst (Fig. 6, left panels). This indicates that in control rats, the maximal tSNA correlated with the transition between late inspiration and post-inspiration. The correlation coefficient (r) for abdominal nerve activity *versus* tSNA was 0.36 ± 0.12 (Fig. 7, left panel). It was noteworthy that in all control WHBPs the correlation between abdominal activity and tSNA occurred during post-inspiration, when the sympathetic activity was decreasing and the abdominal discharge was increasing. In contrast, in the CIH rats ($n = 5$ out of 7) the abdominal nerve activity correlated with the late expiratory phase, occurring prior to phrenic discharge (Fig. 6, right panels). Similar to control rats, maximal tSNA correlated with late inspiration in the CIH group. However, unlike control rats, a second peak in tSNA was found to correlate with the late expiratory peak in abdominal nerve activity ($r = 0.36 \pm 0.11$; Fig. 7, right panel). Two out of 7 CIH preparations did not show significant correlation coefficients during late expiration, despite the fact that these preparations exhibited a greater peak of abdominal nerve activity during late expiration. These were not considered in the data analysis.

Discussion

CIH exposure, hypertension and sympathetic overactivity

The mechanisms underlying the hypertension observed after CIH exposure are not understood completely. It is well characterized that adult rats submitted to CIH for 35 days present an increase in arterial pressure (Fletcher, 2001; Zoccal *et al.* 2007*a*,*b*). However, our study is the first to show that juvenile rats exposed to CIH for just 10 days exhibit a significant increase in baseline arterial pressure comparable to that reported previously in adult rats using a similar protocol of CIH but for 35 days (Zoccal *et al.* 2007*a*,*b*). Combined with this increase in arterial pressure, we observed a different pattern of

sympathetic activity in CIH rats. Both CIH and control groups presented a peak of tSNA during late inspiration with a decline during post-inspiration. However, CIH rats also exhibited an additional significant increase in tSNA during late expiration, which correlated with an enhanced late expiratory activity. It is noteworthy that this difference in the tSNA pattern was not dependent on afferents arising either from the lungs (these are absent in WHBP) or from the carotid bodies, which were removed in some experiments without altering the distinct

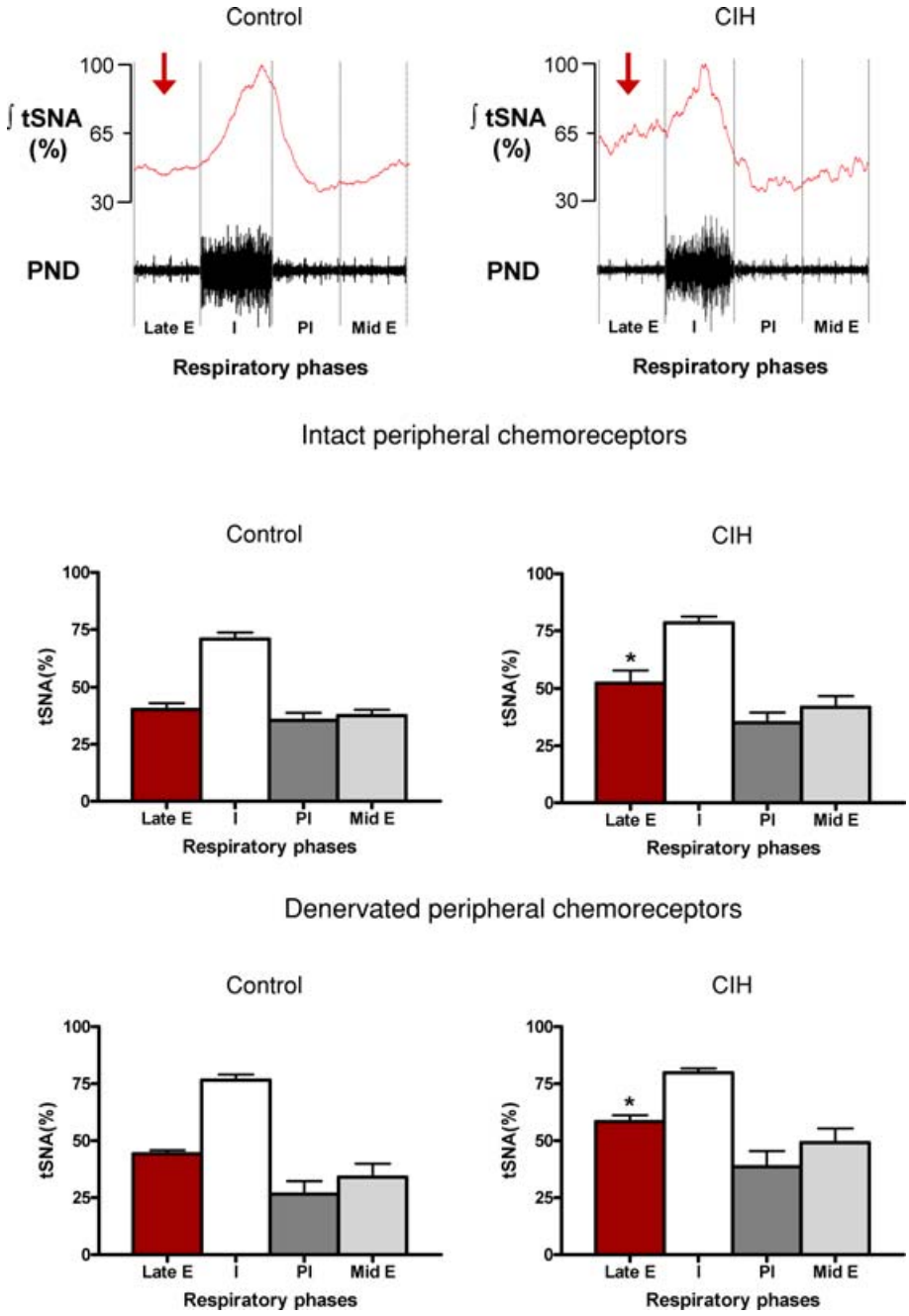

Figure 4. Respiratory–sympathetic coupling assessed in control and CIH-treated rats
Upper panels: phrenic-triggered average of thoracic sympathetic nerve activity (tSNA) obtained from 10 phrenic cycles in a representative control (left) and CIH-treated rat (right). Peak sympathetic activity was normalized to 100% and the noise level to 0%. Note the elevated tSNA in Late E in CIH-treated rats (arrows). Middle panels: mean tSNA during late expiratory (Late E), inspiratory (I), post-inspiratory (PI) and mid-expiratory (Mid E) parts of the respiratory cycle in control ($n = 11$) and CIH ($n = 9$) rats with intact peripheral chemoreceptors. * Different from control, $P < 0.05$. Lower panels: mean tSNA relative to the respiratory cycle in CIH ($n = 5$) and control rats ($n = 3$) with denervated peripheral chemoreceptors. * Different from control, $P = 0.01$.

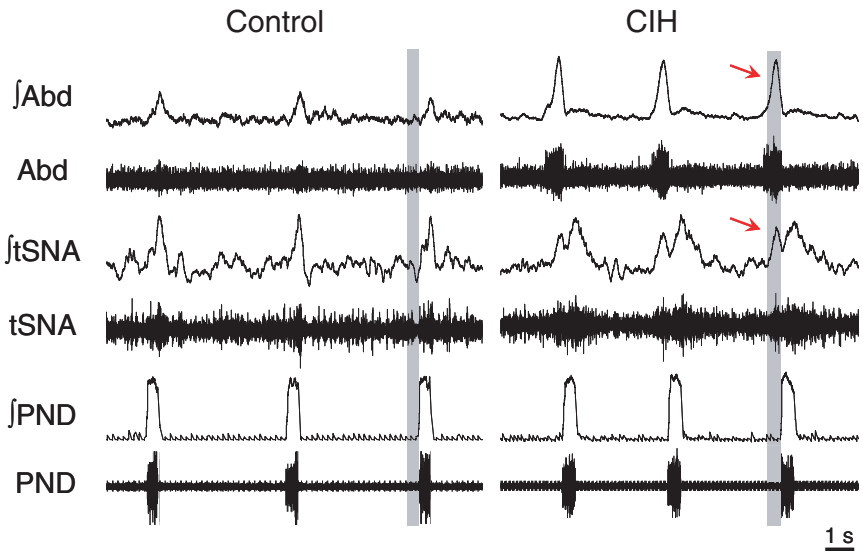

Figure 5. Simultaneous recordings of raw and integrated (∫) abdominal (Abd), thoracic sympathetic (tSNA) and phrenic nerve activities (PND) in a representative control and CIH-treated WHBP (CIH)
The shaded grey area in the recordings represents the late expiratory phase of the respiratory cycle. Note the emergence of late expiratory discharges in both the Abd and tSNA (arrowed) of CIH-treated rats.

pattern and coupling between phrenic and sympathetic activities. Therefore, the observed change in the coupling of respiratory and sympathetic activities reflects a central nervous system phenomenon.

Respiratory pattern after 10 days of CIH exposure

The central respiratory rhythm is generated in the brainstem (Feldman & Smith, 1995; Richter, 1996; Smith *et al.* 2007). Inspiratory and expiratory neurons involved in the generation of the respiratory pattern are predominantly connected reciprocally via inhibitory pathways to produce alternating inspiratory and expiratory spinal and cranial motor activities (Richter, 1996; Richter & Spyer, 2001; Smith *et al.* 2007). In our experiments, no significant changes were observed in inspiratory phrenic activity in CIH rats, indicating that the inspiratory activity was not significantly affected by CIH exposure. On the other hand, the early post-inspiratory activity of the cervical vagus nerve was smaller in CIH than controls. Besides, CIH rats also exhibited a novel peak in the abdominal nerve activity during late expiration, consistent with an

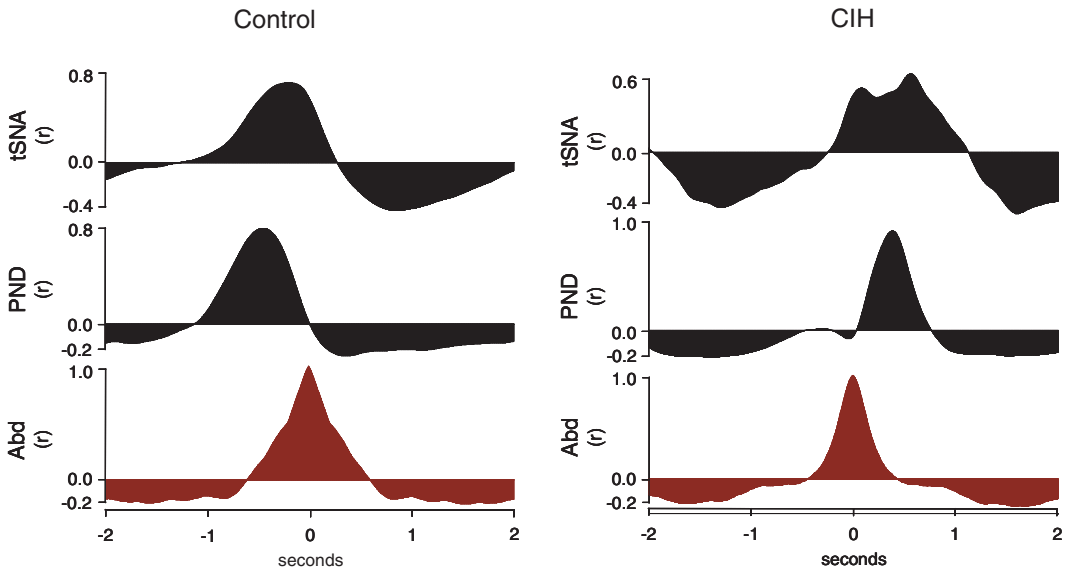

Figure 6. Cross-correlation analyses among the activities of thoracic sympathetic (tSNA, upper panel), phrenic (PND, middle panel) and abdominal (Abd, reference activity) nerves of a representative control and CIH WHBP
PND and tSNA were triggered from the main peak in Abd. In control rats, the main Abd discharge occurred during the post-inspiratory period but in rats treated with CIH this occurred late in the expiratory phase. Note the switch in correlation of Abd to tSNA from post-inspiration in control rats to late expiration in CIH-treated rats.

enhanced or forced expiration. Accordingly, our results indicate that CIH rats exhibit a different pattern of expiratory activity, with reduced post-inspiratory and enhanced late-expiratory activities. We did not determine whether the altered expiratory activity pattern is also observed in *in vivo* preparations but this possibility deserves additional studies.

A major source of expiratory neurons in the respiratory network is the Bötzinger complex (BötC), a neuronal group located in the ventral respiratory column of the ventrolateral medulla (Ezure, 1990; Jiang & Lipski, 1990; Shen *et al.* 2003; Smith *et al.* 2007). The BötC contains neurons that exhibit a decrementing pattern of discharge, characterized by a rapid depolarization at the end of inspiration (post-inspiratory neurons, post-I), and neurons that show an augmenting pattern of discharge (augmenting expiratory neurons, aug-E), which initiate their firing in mid-expiration and terminate prior to phrenic activity (Smith *et al.* 2007). The left panel of Fig. 8 illustrates the interrelationship among the expiratory neurons located in BötC and the other respiratory and autonomic neurons in the ventral medulla. The pattern of activity of post-I neurons can be recorded in cervical vagus and abdominal nerves. Abdominal nerve activity also presents an augmenting pattern of activity during late expiration in conditions of enhanced respiratory drive, such as during the activation of peripheral chemoreceptors (data not shown). It is important to note that the basal abdominal nerve activity of WHBP of CIH (but not control) rats exhibited this aug-E firing, suggesting the possibility that intermittent hypoxia excites and recruits aug-E BötC cells (or any other respiratory neurons associated with forced expiration; see Janczewski & Feldman, 2006; Fortuna *et al.* 2008; right panel of Fig. 8) and that this persists even when CIH is withdrawn. Indeed, Kanjhan *et al.* (1995) showed that the firing frequency of BötC neurons increases in hypoxic conditions. Based on the finding that some of these BötC expiratory neurons have bulbospinal projections (Tian *et al.* 1999), these neurons may provide an excitatory drive to the abdominal motoneurones. Thus, we suggest that this connection may be strengthened by CIH as a result of their repetitive activation. The other evidence that supports the hypothesis that BötC aug-E neurons are more excitable in CIH rats is that the early post-inspiratory activity in vagus nerve activity is depressed. With the reciprocal inhibitory connections between post-I and aug-E (Shen *et al.* 2003), we propose that the CIH-induced excitation of aug-E may depress post-I neuronal activity, reducing its firing per respiratory cycle, as illustrated in the right panel of Fig. 8. This is consistent with our finding of a reduction of PI activity in cervical vagus nerve, although it was observed in the early component. An alternative possibility is that CIH depresses PI neuronal activity which allows aug-E to become predominant. Further experiments are required to check these two possibilities.

Respiratory–sympathetic coupling after 10 days of CIH exposure

The pattern of entrainment between sympathetic and respiratory activities varies according to the species, the nerve recorded and state of the preparation (Gilbey *et al.* 1986; Häbler *et al.* 1994; Jänig & Häbler, 2003; Dick *et al.* 2004). In our experiments, the thoracic sympathetic activity of WHBP of control rats exhibits a phasic increase during the inspiratory phase, with a peak mainly in late inspiration, followed by a decline during the post-inspiratory phase and a tonic activity during the end of expiration. Previous studies documented that the respiratory modulation of sympathetic motor outflow occurs, at least in part, at the level of the brainstem via reticulospinal sympathoexcitatory neurons located in the rostral ventrolateral medulla (RVLM, Barman & Gebber, 1980; McAllen, 1987; Haselton & Guyenet, 1989; Koshiya & Guyenet, 1996; Häbler *et al.* 1996; Zhong *et al.* 1997). Accordingly, neurons involved in the control of respiration could directly modulate the activity of sympathetic RVLM neurons and generate patterns of activity entrained to the respiratory cycle (Haselton & Guyenet, 1989), which are abolished after the inhibition of the medullary respiratory regions including the rostral ventral respiratory group, the pre-Bötzinger complex (pre-BötC) and the BötC (Koshiya & Guyenet, 1996). On the other hand, studies by Mandel & Schreihofer (2006) demonstrated that the activity

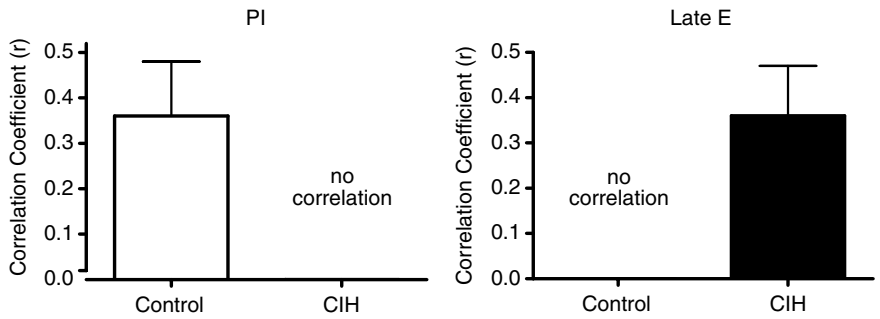

Figure 7. Mean correlation coefficient (*r*) between the activities of thoracic sympathetic and abdominal nerves during post-inspiratory (PI) and late expiratory (Late E) phases in control ($n = 5$) and CIH ($n = 5$) groups
Note the switch in correlation between Abd and tSNA from PI to Late E phase in CIH rats.

of GABAergic neurons of caudal ventrolateral medulla (CVLM) that inhibit the sympathetic RVLM neurons is also modulated by respiratory inputs, suggesting an indirect pathway of respiratory modulation for RVLM neurons. Therefore, based on the data showing that: (i) sympathoexcitatory RVLM neurons exhibit a peak of discharge coincident with the phrenic burst (Haselton & Guyenet, 1989), (ii) GABAergic neurons of CVLM neurons present a depression of the neuronal activity during inspiration or an increase in neuronal discharge during post-inspiration (Mandel & Schreihofer, 2006), and (iii) inspiratory and post-inspiratory neurons are both excitatory and inhibitory (Bianchi *et al.* 1995; Smith *et al.* 2007), a possible scenario for the respiratory–sympathetic coupling observed in control rats is that the activity of RVLM neurons is modulated by inputs from inspiratory and post-inspiratory neurons either directly or via GABAergic CVLM neurons, as illustrated in the left panel of Fig. 8.

With respect to the WHBP of CIH rats, the thoracic sympathetic activity also presented a peak of activity during late inspiration, followed by a decline during post-inspiration. However, CIH rats exhibit a ramping pattern of sympathetic activity during expiration, with a significantly higher activity during the late expiratory phase in comparison to controls. Dick *et al.* (2004)

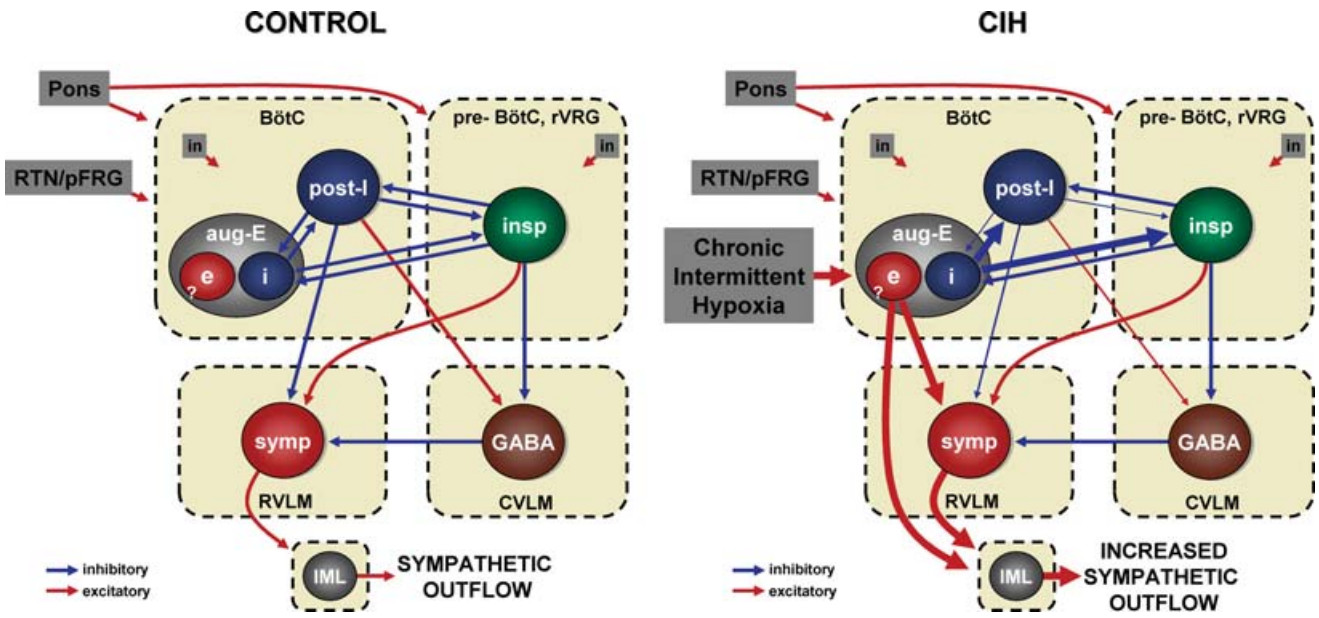

Figure 8. Schematic drawings of the coupling between central respiratory and sympathetic activity in control and CIH rats

In control rats (left panel), expiratory neurons (post-inspiratory, post-I, and inhibitory (i) augmenting expiratory neurons, aug-E), mainly located in Bötzinger complex (BötC; Sun *et al.* 1998; Smith *et al.* 2007), and inspiratory neurons (insp) located in pre-Bötzinger complex (pre-BötC) and rostral ventral respiratory group (rVRG) are reciprocally connected by inhibitory pathways coordinating the respiratory rhythm (Richter, 1996; Tian *et al.* 1999; Richter & Spyer, 2001; Shen *et al.* 2003; Smith *et al.* 2007). The different types of inspiratory neurons recorded in pre-BötC and rVRG were classified together as 'insp' for clarity. The grey boxes represent the main tonic excitatory sources to BötC (intrinsic (in) BötC, Smith *et al.* 2007; retrotrapezoid nucleus/parafacial respiratory group (RTN/pFRG), Janczewski & Feldman, 2006; and pons, Smith *et al.* 2007) and pre-BötC (in pre-BötC (intrinsic, in) and pons, Johnson *et al.* 1994; Smith *et al.* 2007). The sympathetic–respiratory coupling observed in thoracic sympathetic activity in the WHBP of control rats is driven potentially by projections from insp and post-I, modulating the activity of premotor sympathetic neurons (symp) located in rostral ventrolateral medulla (RVLM) directly (Haselton & Guyenet, 1989) or via inhibitory neurons (GABA) located in caudal ventrolateral medulla (CVLM, Mandel & Schreihofer, 2006). In CIH rats (right panel), the excitability of aug-E neurons is probably increased after CIH exposure (indicated by the increased abdominal nerve activity during Late E), which, in turn, may depress the activity of the post-I neurons and consequently reduce the post-inspiratory activity in cervical vagus nerve (as reported herein). In addition, we hypothesize that the excitability of another population of excitatory (e) aug-E neurons is also increased in CIH rats and it may be the source of the neuronal activity that is driving excitatory inputs to symp and sympathetic preganglionic neurons of the intermediolateral column of spinal cord (IML; Sun *et al.* 1997; Tian *et al.* 1999), leading to the enhanced sympathetic activity observed during late expiration. This e aug-E population is speculative (?) and needs to be confirmed as a driver of sympathetic overactivity of CIH rats. No changes in inspiratory activity were observed in CIH possibly because of the reciprocal, and presumed equivalent, changes in aug-E and post-I inhibitory activity on inspiratory neurons.

reported that acute short-term hypoxia (8% O_2 for 30–45 s) increases splanchnic sympathetic nerve activity mainly during the second half of expiration. In another study, Dick *et al.* (2007) also demonstrated that anaesthetized adult rats exposed to acute intermittent hypoxia (10 exposures of 8% O_2 for 45 s) presented an increase in tSNA during the first half of expiration that persisted until 60 min after the last exposure of hypoxia, indicating that acute intermittent hypoxia enhances respiratory–sympathetic coupling. This preferential recruitment of the sympathetic activity in the expiratory phase during hypoxia is consistent with our data in CIH rats. However, these previously reported observations were made either during (Dick *et al.* 2004) or immediately after (Dick *et al.* 2007) the hypoxic stimulus while those in the present study were made in CIH rats 24 h after the last exposure to hypoxia. Our findings suggest that 10 days of CIH induces a long-term and persistent alteration in the strength of central coupling between late expiratory activity and sympathetic motor circuitry in juvenile rats, which is associated with arterial hypertension. In future studies it will be important to determine how long these changes persist after the cessation of the intermittent hypoxia.

The analysis of cross-correlation showed that the increase in tSNA during late expiration correlated with this late expiratory peak of abdominal nerve activity in CIH rats, which was not observed in controls. According to Cohen (1988), this correlation ($r = 0.36 \pm 0.11$) was of medium strength and is considered statistically significant. Our analysis does not allow us to determine whether the enhanced abdominal expiratory activity is directly driving sympathetic activity or vice versa. Alternatively, a common excitatory drive impinging on both abdominal and sympathetic activities may exist. However, based on related evidence, we hypothesize that the enhanced late expiratory activity may be driving the late expiratory burst in tSNA and probably BötC aug-E neurons are modulating RVLM pre-sympathetic neurons. Studies by Thomas *et al.* (2001) have shown that the activation of neurons in the ventral surface of medulla, at the level of BötC and pre-BötC, evoked a reduction in the phrenic nerve discharge accompanied by an increase in arterial pressure, indicating an entrainment between expiration and sympathoexcitation. This is consistent with a study by Sun *et al.* (1997) showing close appositions of axonal projections from intracellularly labelled BötC neurons to RVLM bulbospinal neurons. Additionally, it may also be the case that the enhanced late expiratory discharge in tSNA results from direct projections of aug-E BötC neurons to spinal cord (Tian *et al.* 1999). Therefore, we suggest that the enhanced activity of aug-E neurons and correlated increase in tSNA may occur via projections to RVLM pre-sympathetic neurons and/or spinal cord and that the synaptic strength of this excitatory input(s) is increased by CIH, as illustrated in the right panel of Fig. 8. We also acknowledge that CVLM neurons, which inhibit the RVLM bulbospinal cells, should also be considered as they are also respiratory modulated (Mandel & Schreihofer, 2006).

Conclusion and perspectives

In conclusion, our findings show that juvenile rats exposed to CIH for 10 days exhibit hypertension and an increase in sympathetic activity that correlates with an enhanced/forced expiration. Thus, our data indicate that CIH induces chronic changes in neuronal plasticity in the coupling between respiratory and sympathetic activities in this experimental model. We have not yet been able to determine whether the enhanced sympathetic activity observed during late expiration is the cause of hypertension observed in CIH rats. This is an important issue that deserves further electrophysiological studies to verify possible changes in the neurochemical profile of neurons of the ventral medulla involved in the generation of sympathetic and respiratory activities.

References

Adrian ED, Bronk DW & Phillips G (1932). Discharges in mammalian sympathetic nerves. *J Physiol* **74**, 115–133.

Anrep GV, Pascual W & Rössler R (1936). Respiratory variations of the heart rate I. The reflex mechanism of the respiration arrhythmia. *Proc R Soc Lond B Biol Sci* **119**, 191–217.

Barman SM & Gebber GL (1980). Sympathetic nerve rhythm of brain stem origin. *Am J Physiol Regul Integr Comp Physiol* **239**, R42–R47.

Bianchi AL, Denavit-Saubié M & Champagnat J (1995). Central control of breathing in mammals: neuronal circuitry, membrane properties, and neurotransmiters. *Physiol Rev* **75**, 1–45.

Boczek-Funcke A, Dembowsky K, Habler HJ, Janig W, McAllen RM & Michaelis M (1992). Classification of preganglionic neurones projecting into the cat cervical sympathetic trunk. *J Physiol* **453**, 319–339.

Braga VA, Soriano RN & Machado BH (2006). Sympathoexcitatory response to peripheral chemoreflex activation is enhanced in juvenile rats exposed to chronic intermittent hypoxia. *Exp Physiol* **91**, 1025–1031.

Caples SM, Gami AS & Somers VK (2005). Obstructive sleep apnea. *Ann Intern Med* **142**, 187–197.

Cohen J (1988). *Statistical Power Analysis for the Behavioral Sciences*, 2nd edn. Lawrence Erlbaum Associates, Hillsdale, NJ, USA.

Dick TE, Hsieh Y-H, Morrison S, Coles SK & Prabhakar N (2004). Entrainment pattern between sympathetic and phrenic nerve activities in the Sprague-Dawley rat: hypoxia-evoked sympathetic activity during expiration. *Am J Physiol Regul Integr Comp Physiol* **286**, R1121–R1128.

Dick TE, Hsieh YH, Wang N & Prabhakar N (2007). Acute intermittent hypoxia increases both phrenic and sympathetic nerve activities in the rat. *Exp Physiol* **92**, 87–97.

Ezure K (1990). Synaptic connections between medullary respiratory neurons and considerations on the genesis of respiratory rhythm. *Prog Neurobiol* **35**, 429–450.

Feldman JL & Smith JC (1995). Neural control of respiratory pattern in mammals: An overview. In *Regulation of Breathing*, ed. Dempsey JA & Pack AI, pp. 39–69. Decker, New York.

Fletcher EC (2001). Physiological consequences of intermittent hypoxia: systemic blood pressure. *J Appl Physiol* **90**, 1600–1605.

Fortuna MG, West GH, Stornetta RL & Guyenet PG (2008). Botzinger expiratory-augmenting neurons and the parafacial respiratory group. *J Neurosci* **28**, 2506–2515.

Gilbey MP, Numao Y & Spyer KM (1986). Discharge patterns of cervical sympathetic preganglionic neurones related to central respiratory drive in the rat. *J Physiol* **378**, 253–265.

Greenberg HE, Sica AL, Scharf SM & Ruggiero DA (1999). Expression of c-fos in the rat brainstem after chronic intermittent hypoxia. *Brain Res* **816**, 638–645.

Häbler H-J, Bartsch T & Jänig W (1996). Two distinct mechanisms generate the respiratory modulation in fibre activity of the rat cervical sympathetic trunk. *J Auton Nerv Syst* **61**, 116–122.

Häbler H-J, Jänig W & Michaelis M (1994). Respiratory modulation in the activity of sympathetic neurones. *Prog Neurobiol* **43**, 567–606.

Haselton JR & Guyenet PG (1989). Central respiratory modulation of medullary sympathoexcitatory neurons in rat. *Am J Physiol Regul Integr Comp Physiol* **256**, R739–R750.

Hoffmann M, Bybee K, Accurso V & Somers VK (2004). Sleep apnea and hypertension. *Minerva Med* **95**, 281–290.

Janczewski WA & Feldman JL (2006). Distinct rhythm generators for inspiration and expiration in the juvenile rat. *J Physiol* **570**, 407–420.

Jänig W & Häbler H-J (2003). Neurophysiological analysis of target-related sympathetic pathways – from animal to human: similarities and differences. *Acta Physiol Scand* **177**, 255–274.

Jiang C & Lipski J (1990). Extensive monosynaptic inhibition of ventral respiratory group neurons by augmenting neurons in the Bötzinger complex in the cat. *Exp Brain Res* **81**, 639–648.

Johnson SM, Smith JC, Funk GD & Feldman JL (1994). Pacemaker behavior of respiratory neurons in medullary slices from neonatal rat. *J Neurophysiol* **76**, 2598–2608.

Kanjhan R, Lipski J, Kruszewska B & Rong W (1995). A comparative study of pre-sympathetic and Bötzinger neurons in the rostral ventrolateral medulla (RVLM) of the rat. *Brain Res* **699**, 19–32.

Kline DD, Ramirez-Navarro A & Kunze DL (2007). Adaptive depression in synaptic transmission in the nucleus of the solitary tract after in vivo chronic intermittent hypoxia: evidence for homeostatic plasticity. *J Neurosci* **27**, 4663–4673.

Koshiya N & Guyenet PG (1996). Tonic sympathetic chemoreflex after blockade of respiratory rhythmogenesis in the rat. *J Physiol* **491**, 859–869.

Leuenberger UA, Brubaker D, Quraishi S, Hogeman CS, Imadojemu VA & Gray KS (2005). Effects of intermittent hypoxia on sympathetic activity and blood pressure in humans. *Auton Neurosci* **121**, 87–93.

Ling L, Fuller DD, Bach KB, Kinkead R, Olson EB & Mitchell GS (2001). Chronic intermittent hypoxia elicits serotonin-dependent plasticity in the central neural control of breathing. *J Neurosci* **21**, 5381–5388.

McAllen RM (1987). Central respiratory modulation of subretrofacial bulbospinal neurones in the cat. *J Physiol* **388**, 533–545.

McGuire M, Zhang Y, White DP & Ling L (2003). Chronic intermittent hypoxia enhances ventilatory long-term facilitation in awake rats. *J Appl Physiol* **95**, 1499–1508.

Malpas S (1998). The rhythmicity of sympathetic nerve activity. *Prog Neurobiol* **56**, 65–96.

Mandel DA & Schreihofer AM (2006). Central respiratory modulation of barosensitive neurones in rat caudal ventrolateral medulla. *J Physiol* **572**, 881–896.

Narkiewicz K & Somers VK (1997). The sympathetic nervous system and obstructive sleep apnea: implications for hypertension. *J Hypertens* **15**, 1613–1619.

Pickering AE & Paton JFR (2006). A decerebrate, artificially-perfused in situ preparation of rat: utility for the study of autonomic and nociceptive processing. *J Neurosci Methods* **155**, 260–271.

Pilowsky P (1995). Good vibrations? Respiratory rhythms in the central control of blood pressure. *Clin Exp Pharmacol Physiol* **22**, 594–604.

Reeves SR, Gozal E, Guo SZ, Sachleben LR Jr, Brittian KR, Lipton AJ & Gozal D (2003). Effect of long-term intermittent and sustained hypoxia on hypoxic ventilatory and metabolic responses in the adult rat. *J Appl Physiol* **95**, 1767–1774.

Reeves SR, Guo SZ, Brittian KR, Row BW & Gozal D (2006). Anatomical changes in selected cardio-respiratory brainstem nuclei following early post-natal chronic intermittent hypoxia. *Neurosci Lett* **402**, 233–237.

Richter DW (1996). Neural regulation of respiration: rhythmogenesis and afferent control. In *Comprehensive Human Physiology*, vol. II, ed. Gregor R & Windhorst U, pp. 2079–2095. Springer-Verlag, Berlin.

Richter DW & Spyer KM (2001). Studying rhythmogenesis of breathing: comparison of *in vitro* and *in vivo* models. *Trends Neurosci* **24**, 464–472.

Shen LL, Li YM & Duffin J (2003). Inhibitory connections among rostral medullary expiratory neurons detected with cross-correlation in the decerebrate rat. *Pflugers Arch* **446**, 365–372.

Simms A, Paton JFR & Pickering AE (2007). Hierarchical recruitment of the sympathetic and parasympathetic limbs of the baroreflex in normotensive and spontaneously hypertensive rats. *J Physiol* **579**, 473–486.

Smith JC, Abdala APL, Koizumi H, Rybak IA & Paton JFR (2007). Spatial and functional architecture of the mammalian brainstem respiratory network: a hierarchy of three oscillatory mechanisms. *J Neurophysiol* **98**, 3370–3387.

Sun Q-J, Goodchild AK, Chalmers JP & Pilowsky PM (1998). The pre-Bötzinger complex and phase-spanning neurons in the adult rat. *Brain Res* **809**, 204–213.

Sun Q-J, Minson J, Llewellyn-Smith IJ, Arnolda L, Chalmers J & Pilowsky P (1997). Botzinger neurons project towards bulbospinal neurons in the rostral ventrolateral medulla of the rat. *J Comp Neurol* **388**, 23–31.

Thomas T, Ralevic V, Bardini M, Burnstock G & Spyer KM (2001). Evidence for the involvement of purinergic signalling in the control of respiration. *Neuroscience* **107**, 481–490.

Tian GF, Peever JH & Duffin J (1999). Bötzinger-complex, bulbospinal expiratory neurones monosynaptically inhibit ventral-group respiratory neurones in the decerebrate rat. *Exp Brain Res* **124**, 173–180.

Zhong S, Zhou SY, Gebber GL & Barman SM (1997). Coupled oscillators account for the slow rhythms in sympathetic nerve discharge and phrenic nerve activity. *Am J Physiol Regul Integr Comp Physiol* **272**, R1314–R1324.

Zhou S-Y & Gilbey MP (1992). Respiratory-related activity of lower thoracic and upper lumbar sympathetic preganglionic neurones in the rat. *J Physiol* **451**, 631–642.

Zoccal DB, Bonagamba LG, Antunes-Rodrigues J & Machado BH (2007*a*). Plasma corticosterone levels is elevated in rats submitted to chronic intermittent hypoxia. *Auton Neurosci* **134**, 115–117.

Zoccal DB, Bonagamba LG, Oliveira FR, Antunes-Rodrigues J & Machado BH (2007*b*). Increased sympathetic activity in rats submitted to chronic intermittent hypoxia. *Exp Physiol* **92**, 79–85.

Acknowledgements

In Brazil this study was supported by CNPq (472704/2004-4) and FAPESP (2004/03285-7 and 2006/51159-6). In the UK J.F.R.P. was in receipt of a Royal Society Wolfson Research Merit Award and A.E.P. holds a Wellcome Trust Advanced Fellowship. The authors thank Dr Ana Paula Lima Abdala for her important contribution to the analyses of the correlograms.